MULTI-SCALE CONTACT MODEL FOR ROUGH CONTACTS

D.K. Karupannasamy[1*], M.B. de Rooij[2] and D.J. Schipper[3]

[1] *Materials innovation institute (M2i) - P.O. box 5008 - 2600 GA Delft - The Netherlands.*

[2,3] *University of Twente, Faculty of Engineering Technology, Laboratory for Surface Technology and Tribology - P.O. box 217 - 7500 AE Enschede - The Netherlands.*

Abstract

In Finite Element (FE) simulations of sheet metal forming (SMF), the coefficient of friction is generally expressed as a constant Coulomb friction. However in reality, the coefficient of friction at the local contact spot varies with the varying operational, deformation and contact conditions. Therefore, it is important to calculate the coefficient of friction under local conditions to better evaluate the formability of the product. Friction at the local contact spot is largely influenced by the micro-mechanisms occurring at asperity level like shearing in the boundary layer, ploughing, surface deformation of the workpiece and hydrodynamic lubrication. In this paper, a multi-scale contact model is developed for the predicting the friction occurring in SMF processes. The model describes the ploughing phenomenon between the workpiece and the tool which is predominant amongst the other friction mechanisms. The change occurring in the surface topography of the workpiece during the deep drawing processes influences the ploughing process. An asperity flattening model for ideal plastic conditions is used to describe this phenomenon. The developed model is analyzed with various workpiece and tool surfaces. The result shows that the coefficient of friction is very much dependent on the surface topography of the interacting surfaces at low nominal contact pressures. At high nominal contact pressures, the surface topography influences less on the friction. The coefficient of friction is also compared on tool surfaces with different roughness, bandwidth and surface lay. The coefficient of friction is found to be high for rough, low bandwidth and transversal anisotropic tool surfaces.

Keywords: Deep drawing; friction modeling; ploughing; multi-scale; deterministic model.

*Corresponding author: D.K.Karupannasamy (d.karupannasamy@m2i.nl)

1. INTRODUCTION

In tribological problems, the traditional contact models of [1] and [2] are characterized by elastically and plastically deforming asperities for small fraction of contact area at one roughness scale. However in the SMF processes, the contact occurs between a smooth tool and rough workpiece surface. The workpiece surface deforms under bulk strain and normal loading which increases the fractional contact area. The contact occurs at two different roughness levels. At workpiece roughness level, the workpiece surface is deformed by normal loading of the tool and stretching of the sheet by the punch. At tool roughness level, tool asperities plough through workpiece due to sliding of sheet between the tools. Ploughing occurs when there is a difference in the hardness of the material under contact. The harder material indents into the softer material and ploughs. The friction force is produced due to the energy losses in deforming the softer surface.

Greenwood and Williamson [1] described an elastic contact model using statistical properties of the surface for the contact between nominally flat surfaces. The surface is assumed to have asperities with a constant radii and known summit density. The asperity based contact models are suitable for a low fraction of area in contact. Pullen and Williamson [2] described a surface based plastic contact model assuming volume conservation. In this model, the asperity flattening process at high loads with rise of asperities is modeled using statistical properties of the surface. Nayak [3] modeled plastic contact with the distribution of contact patches and holes for the given separation using the statistical properties of the surface. He also found that the summit based models do not give the true contact area and the fractional contact area exceeds unity. However, Nayak's analysis was focused at the development of contact patches. He did not explain the detailed shape of the micro contact patches which is critical for the friction prediction due to ploughing effects. Westeneng [4] developed a statistical contact model based on energy and volume conservation. He described the flattening and rising of asperities under plastic loading conditions. He also used the strain deformation models of Wilson and Sheu [5] and Sutcliffe [6] for contact area evolution due to bulk strain. Hol et al., [7] developed the numerical framework for the contact model of Westeneng [4] and

applied it to large scale FE simulations. Ma et al., [8] developed a deterministic model by characterizing the micro contact patches to predict the coefficient of friction in an extrusion process due to ploughing of tool asperities through the extrudate. In their model, the contact between a flat soft surface and a rough hard surface was assumed. The characterization of micro contact patches is adopted from the work of Masen et al., [9] for plastically deforming asperities in sliding contacts.

In this work, a multi-scale contact model is developed for rough contact situations between tool and workpiece in metal forming processes. The model includes the roughnesses of both the sheet and the tool. The developed model combines the approaches of Westeneng [4] and Ma et al., [8] for describing the coefficient of friction in a SMF processes. Results will be presented for several combinations of workpiece and tool surfaces at different separation levels, so the different nominal contact pressures. It will be shown that the calculated coefficient of friction is very much dependent on the separation and the detailed surface topography of the two contacting rough surfaces, so the workpiece and tool surfaces.

2. DETERMINISTIC CONTACT MODEL

A deterministic ploughing model was developed by Ma et al., [8] for an aluminum extrusion process. The contact model includes only one roughness scale (tool roughness). In an aluminum extrusion process, the workpiece is soft and at high loads it deforms onto the tool roughness resulting in a very high fractional contact area. However in SMF processes, the fractional contact area is typically lower. Therefore, it is critical to include both the roughness scales to predict the friction.

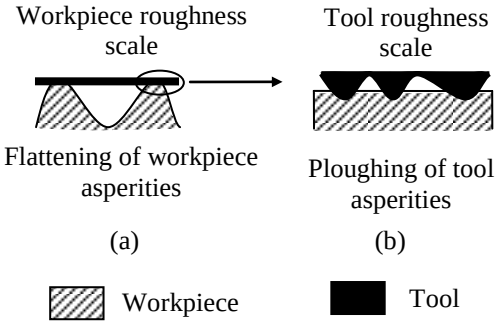

Figure 1 : *Contact between workpiece and tool at (a) workpiece roughness scale and (b) tool roughness scale.*

The multi-scale contact model is developed based on the work of [4] and [8] and applied to SMF processes. The two scales are based on the roughness of the tool and workpiece surfaces. In the workpiece roughness scale, the workpiece is assumed to be rough and the tool to be flat. The smooth tool flattens the encountered workpiece asperities as shown in Fig. 1(a).

At the largest length scale (workpiece roughness scale), the statistical model of Westeneng [4] is used to calculate the flattening of workpiece surface due to normal loading and bulk strain. At tool roughness scale, the tool is assumed to be composed of micro contacts ploughing through the plateaus on the workpiece surface as shown in Fig. 1(b). The deterministic approach is used to model the size and shape of the ploughing tool asperities as described by Ma et al., [8]. The basic process in this model can be summarized as, (see also Fig. 2)

1. Input of representative tool and workpiece surfaces
2. Calculation of the workpiece surface deformed by plastic loading and bulk strain
3. Contact patch identification of the workpiece
4. Mapping of tool asperities onto the identified contact patches
5. Tool asperity shape characterization
6. Tool indentation calculation by force equilibrium
7. Friction calculation

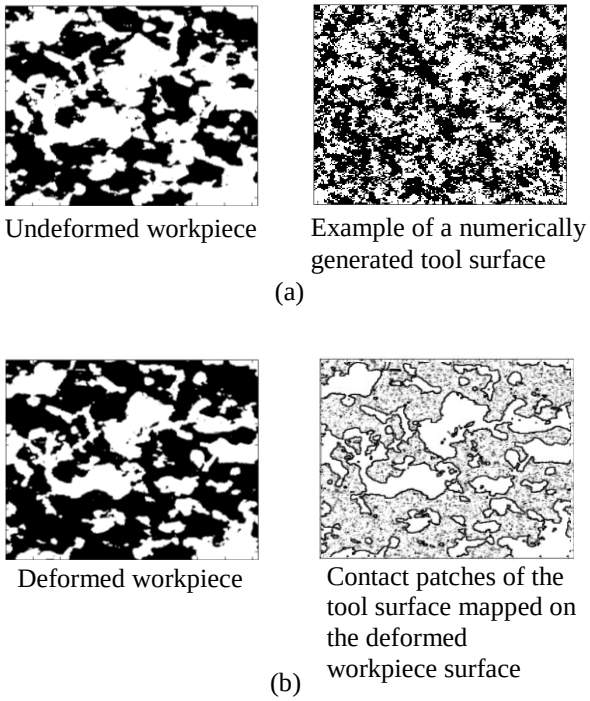

Figure 2 : *(a) Representative workpiece and tool surfaces (1x1mm^2) and (b) Deformed workpiece surface and mapped tool surface.*

The representative workpiece surface is taken from the DC06 steel sheet using confocal microscope. The tool surfaces are digitally generated by using FFT techniques of Hu and Tonder [10] with different values for the roughness parameters. After the input of the surfaces shown in Fig. 2(a), the flattening model of [4]

is used to calculate the deformation of the workpiece surface for ideal plastic conditions. The tool contact patches are identified at the given separation distance using the binary image processing techniques. Each contact patch is identified by a cluster of pixels connected to its edge. Using the 4-connectivity criterion (4 pixels connected together makes a contact patch) contact patches are identified. The pixels which do not make a contact patch are wiped out.

The identified contact patches mapped on the tool surface are shown in Fig. 2(b). The surface heights are extracted from the given surface distribution of the tool surface. Given the tool surface height data of a contact patch, a paraboloid is constructed with an elliptical base of equal volume of the contact patches above the given tool indentation level. Thus each asperity of the tool coming into contact with the workpiece is uniquely characterized for a given tool indentation depth. The contribution of the ploughing forces to the total friction force is dependent on the attack angle here represented by, β_e. The attack angle of an asperity is separately calculated for each asperity depending on the orientation of the elliptical base shape, φ with respect to the sliding direction as shown in Fig. 3. Hokkirigawa and Kato [11] extended the application of 2D slipline model of Challen and Oxley [12] to 3D scenario by introducing a shape factor χ which was determined experimentally. The effective attack angle of an asperity, β_e was given by Ma et al., [8] depending on the orientation of the elliptical base with respect to sliding direction as,

$$\beta_e = 2\arctan\left(\frac{h\sqrt{b^2\cos^2\varphi + a^2\sin^2\varphi}}{\chi ab}\right) \qquad \text{(Eq 1)}$$

where h represents the indentation depth of the tool, a the major radius of the contact ellipse, b the minor radius of the contact ellipse, φ the orientation of the contact ellipse, χ the shape factor of the asperity, (χ = 0.8).

The tool indentation depth is calculated by means of iterative procedure. The total applied load should be carried by all the tool asperities which are in contact with workpiece. In the model, it is assumed that only front half of the asperity is in contact when sliding for plastic contact conditions. The load carried by an elliptical paraboloid under plastic conditions according to [9] is given as,

$$F_p = \pi H h\sqrt{ab} \qquad \text{(Eq 2)}$$

where H represents the hardness of the interface.

An average effective attack β_{avg} angle is calculated by means of weighting the effective attack angle of individual asperity with its contact area of the mirco contacts as follows,

$$\beta_{avg} = \frac{\sum_{i=1}^{m} \beta_e^i A_{cp}^i}{\alpha A_{nom}} \qquad \text{(Eq 3)}$$

where m represents the number of tool asperities in contact, A_{cp} the area of the tool contact patch, α the fractional contact area, A_{nom} the nominal contact area of the interface.

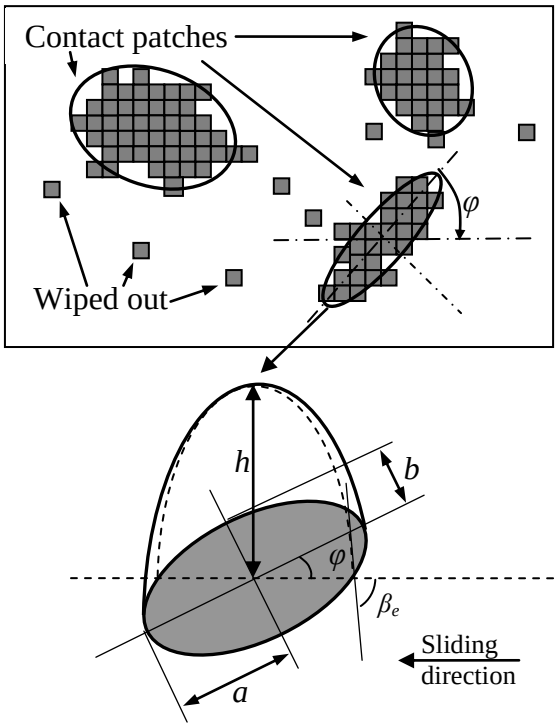

Figure 3: *Identification and characterization of tool asperities from Ma et al [8].*

3. RESULTS

For the calculations, workpiece surfaces are measured from three different spots of size 1x1 mm with a spatial resolution of 1 µm using a confocal microscope. For parametric study, various tool surfaces with different surface properties are digitally generated with the roughness properties as listed in Table 1. The calculated coefficient of friction is shown in Fig. 4(a), 5 and 6 for various dimensionless separations. The results are also shown for three different workpiece spots. The friction values are shown for various tool roughness, R_q, surface lay, γ and bandwidth parameter, Ψ. The surface lay is defined by the ratio of autocorrelation length of the surface in X and Y direction. The bandwidth parameter is defined by the moments of power spectral density of the surface as,

$$\psi = \frac{m_0 m_4}{m_2^2} = \frac{\sigma_z \sigma_\kappa}{\sigma_s^2} \qquad \text{(Eq 4)}$$

where σ_z represents the standard deviation of the surface height, σ_κ the standard deviation of the surface curvature, σ_s the standard deviation of the surface slope.

Table 1: *Tool surface parameters used in the calculation.*

Tool surface	R_q [µm]	γ [-]	Ψ [-]
1	1	1	6
2	2	1	6
3	0.5	1	6
4	1	0.1	6
5	1	9	6
6	1	1	3
7	1	1	12

The calculated coefficient of friction is compared for tool surface 1 of three different roughness shown in Fig. 4(a). For rough tool surfaces, the asperities plough with a high contact angle through the workpiece surface. Hence, the coefficient of friction is high. However for smooth tool surfaces, the asperities are more blunt which results in a low coefficient of friction. It can also be seen that if the same tool is in contact with different workpiece surfaces, the coefficient of friction shows different trends. The difference can be explained with the formation of contact patches with workpiece. The average contact area of a patch (Total contact area / number of contact patches) of the tool surface 1 with the different workpiece surfaces is shown in Fig. 4(c). For the workpiece surface with low number of contact patches (Workpiece surface 3), tool indentation into the workpiece has to be high to balance the applied load. For the case of a high number of contact patches (Workpiece surface 1), a low value of tool indentation is sufficient to balance the applied load. At low indentation depths as shown in Fig. 4(b), the tool asperities cluster to form only small contact patches with high contact angle. This results in sharper tool asperities and results in a high coefficient of friction.

When the separation reduces (or the nominal contact pressure increases), the average area of a contact patch decreases slower for workpiece surface 1 than the other surfaces as shown in Fig. 4(c). This means that workpiece forms big contact patches in low numbers. This allows existing tool contact patches to grow bigger. This clustering of asperities results in the formation of blunt contact patches. Hence the coefficient of friction reduces with the separation for workpiece surface 1 when compared with workpiece surface 3 for the same tool surface. For workpiece surface 3, the average area of a contact patch is lower than workpiece surface 1 with the decrease in separation as shown in Fig. 4(c). This means that small

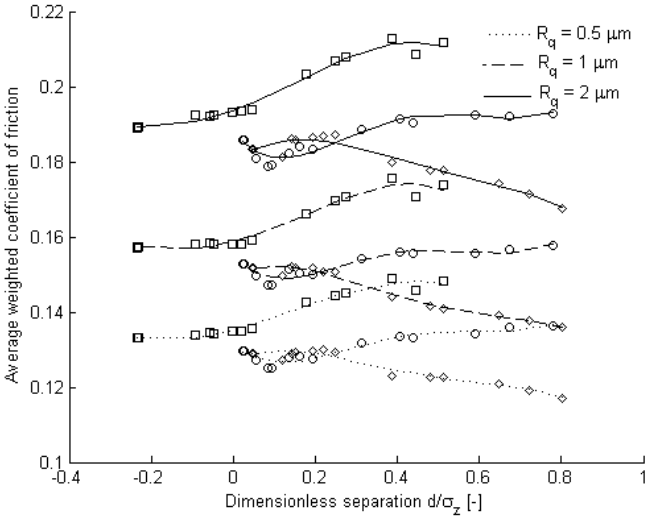

□ , ○ and ◇ - Workpiece surface 1, 2 and 3

(a)

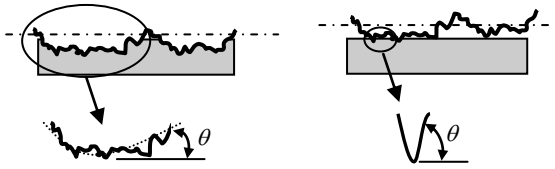

High indentation Low indentation

(b)

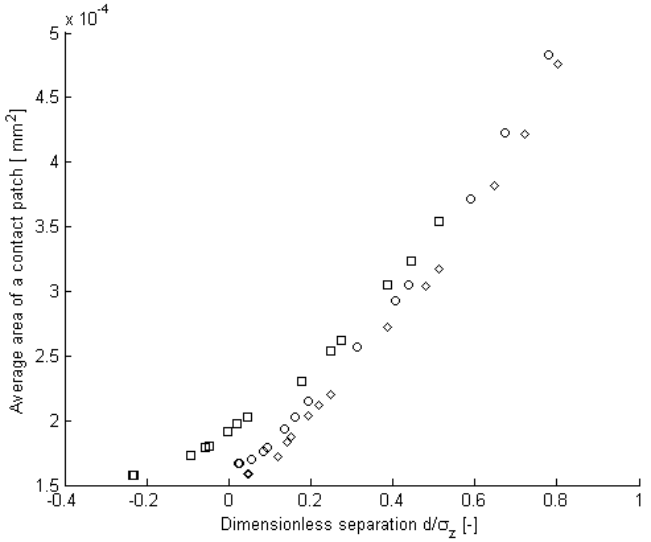

□ , ○ and ◇ - Workpiece surface 1, 2 and 3

(c)

Figure 4: *(a) Calculated coefficient of friction for various workpiece surfaces with various tool surfaces of different roughness, (b) Clustering of asperities at high and low separations and (c) Average contact area of a patch of the tool surface 1 with various workpiece surfaces.*

new contact patches are formed. This also allows tool to form new contact patches with sharp contact angles

which results in increase of the friction. However, for workpiece surface 2 even with lower average area of a contact patch, the coefficient of friction shows same trend as workpiece surface 1. The reason could be that there is a balance in the growth of size and number of contact patches. The growth of contact patches in workpiece surface highly influences the trend of the coefficient of friction. At high separations, the coefficient of friction is more dependent on the detailed micro geometry as compared to low values for the separation. Calculated dimensionless separation levels for a deep drawing process at a given normal load is shown in the Fig. 5. The dimensionless separation between the tool and workpiece reduces due to the application of the contact pressure. At high bulk strain levels, the material becomes softer and hence the separation levels decrease further.

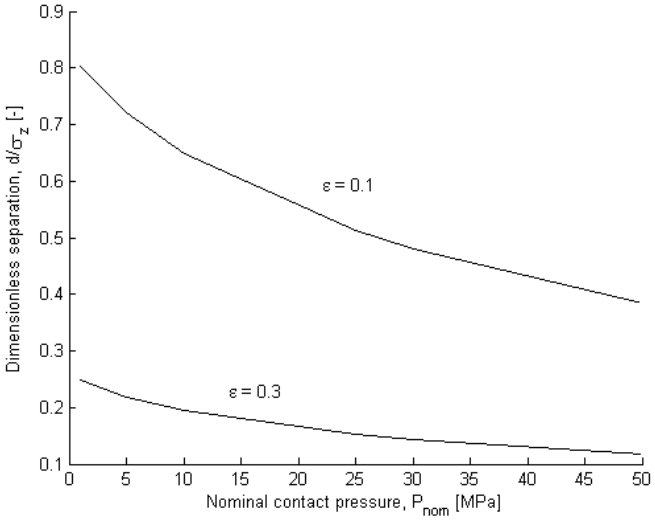

Figure 5: *Calculated separation levels for a given normal load in a deep drawing process.*

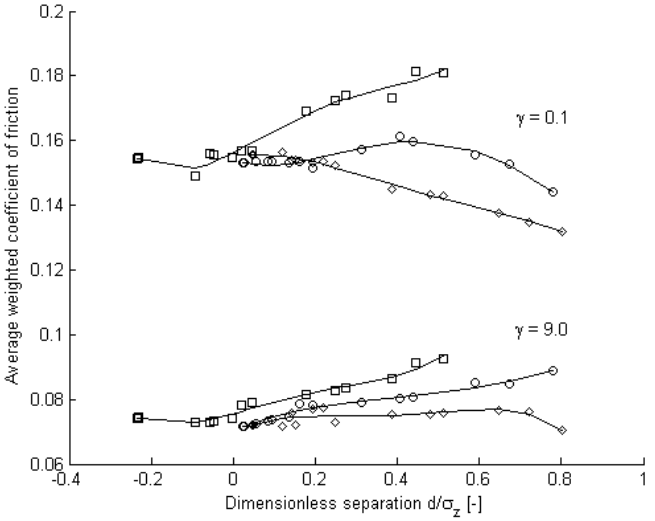

□ , ○ and ◇ - Workpiece surface 1, 2 and 3

Figure 6: *Calculated coefficient of friction for various workpiece surfaces in contact with tool surfaces of transversal and longitudinal surface lay.*

In Fig. 6, the coefficient of friction is shown for transverse and longitudinal lay. A transverse lay results in sharper contacts with respect to the sliding direction and produces high friction. A longitudinal lay results in blunt contacts and results in a low friction level. In Fig. 7, the results from the surfaces of low and high bandwidth parameters, Ψ are shown. Low bandwidth surfaces (spiky surfaces) results in a higher coefficient of friction than high bandwidth surfaces (smooth surfaces).

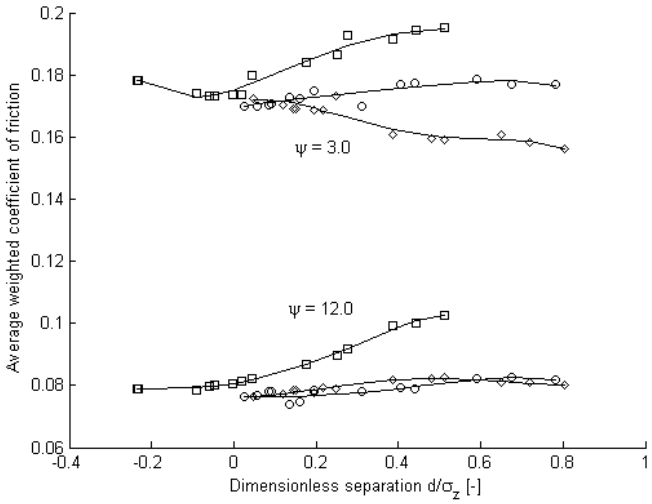

□ , ○ and ◇ - Workpiece surface 1, 2 and 3

Figure 7: *Calculated coefficient of friction for various workpiece surfaces with tool surfaces of high and low bandwidth parameters.*

4. Conclusion

A multi-scale contact model is developed for contact occurring in SMF processes for describing the friction at the local contact conditions under boundary lubrication regime. The model combines the surface deformation of the workpiece due to normal loading and eventually plastic bulk strain with a detailed geometrical description of the tool asperities ploughing through the sheet surface. Results are shown for various combinations of tool and workpiece surfaces. It has been shown that the calculated coefficient of friction is strongly dependent on the microgeometry of the tool and the workpiece, in particular at low values of the nominal contact pressure. At high nominal pressure, the coefficient of friction approaches to same value irrespective of the workpiece surface. Further it has been found that a rougher tool surface results in a higher coefficient of friction. A transverse surface lay produces higher coefficient than longitudinal surface lay. Also a low bandwidth tool surface (spiky surface) results in a higher coefficient of friction as compared to high bandwidth surface. The magnitude of the coefficient of friction values is reasonable according to the experimental knowledge.

Acknowledgments

This research was carried out under the project number MC1.07289 in the framework of the Research Program of the Materials innovation institute, The Netherlands (www.m2i.nl).

5. References

1. J.A. Greenwood and J.B.P Williamson, Contact of nominally flat surfaces, Proceedings of the Royal Society of London. Series A, Mathematical and Physical sciences 295 (1966) 300–319.
2. J. Pullen and J.B.P Williamson, On the plastic contact of rough surfaces, Proceedings of the Royal Society of London. Series A, Mathematical and Physical sciences 327 (1972) 159–173.
3. P. Nayak, Random Process Model of Rough Surfaces in Plastic Contact, Wear, Vol. 26 (1973) 305–333.
4. J. Westeneng, Modelling of contact and friction in deep drawing processes, Ph.D. thesis, University of Twente, The Netherlands, 2001.
5. W.R.D Wilson and S. Sheu, Real area of contact and boundary friction in metal forming, International Journal of Mechanical Sciences 30 (1988) 475–489.
6. M.P.F Sutcliffe, Surface Asperity Deformation in Metal Forming Processes, International Journal of Mechanical Sciences, Vol. 30 No. 11 (1988) 848 – 867.
7. J. Hol, M.V. Cid Alfaro, M.B. de Rooij and T. Meinders, Advanced friction modeling for sheet metal forming, Wear (2011), doi:10.1016/j.wear.2011.04.004
8. X. Ma, , M.B. de Rooij, and D.J. Schipper, A load dependent friction model for fully plastic contact conditions. Wear, Vol. 269(11-12) (2010), 790-796.
9. M.A Masen, M.B de Rooij and D.J. Schipper, Micro-contact based modelling of abrasive wear, Wear, Vol 258(2005), 339-348.
10. Y.Z. Hu, and K Tonder, Simulation of 3-D Random Rough Surface by 2-D Digital Filter and Fourier Analysis, International Journal of Machine Tools and Manufacture, Vol. 32 (1992) 83-90.
11. K. Hokkirigawa, and K. Kato, An Experimental and Theoretical Investigation of Ploughing, Cutting and Wedge Formation During Abrasive Wear, Tribology International, Vol. 21 (1988) 51-57.
12. J.M. Challen, and P.L.B. Oxley, An explanation of the Different Regimes of Friction and Wear Using Asperity Deformation Models, Wear, Vol. 53 (1979) 229 - 243.